1

2

3

4

5 **Drop-on-demand printing of personalised orodispersible films fabricated by precision**

6 **micro-dispensing**

7

8 Chak Tam[1], Matthew Alexander[2], Peter Belton,[3] Sheng Qi[1*]

9 1. School of Pharmacy, University of East Anglia, Norwich, UK

10 2. School of Engineering, University of East Anglia, Norwich, UK

11 3. School of Chemistry, University of East Anglia, Norwich, UK

12

13

14

15

16

17

18

19 **Corresponding author: sheng.qi@uea.ac.uk**

20

21

22

23

24

25

26

27

28

29

30

31

32

33

34

35 **Abstract:**

36 Personalised orodispersible films (ODFs) manufactured at the point of care offer the possibility

37 of adapting the dosing requirements for individual patients. Inkjet printing was extensively

38 explored as a tool to produce personalised ODFs, but it is extensively limited to dispensing

39 liquid with low viscosity and the interaction between ink and edible substrate complicates the

40 fabrication process. In this study, we evaluated the feasibility of using a micro-dispensing (MD)

41 jet system capable of accurately dispensing viscous liquid to fabricate substrate-free ODFs on-

42 demand. The model inks containing hydroxypropyl methylcellulose (HPMC) and paracetamol

43 were used to prepare personalised ODFs by expanding the film area. Cast films were used as

44 the control sample to benchmark the mechanical properties, disintegration time, and dosing

45 accuracy of MD printed ODFs. Both the cast and printed film showed smooth surface

46 morphology without any bubbles. No significant difference was found in the disintegration

47 time of the MD printed films compared to the cast films. High precision in dosing by MD

48 printing was achieved. The dose of paracetamol had a linear correlation with the dimension of

49 the printed films (R^2 = 0.995). The results provide clear evidence of the potential of MD

50 printing to fabricate ODFs and the knowledge foundation of advancing MD printing to a point-

51 of-care small-batch manufacturing technology of personalised ODFs.

52

53 **Keywords:**

54 orodispersible film, personalised medicine, micro-dispensing, 3D printing, drop-on-demand,

55 solid dosage form

1. Introduction

Orodispersible films have gained popularity in the last decade as an alternative solid dosage form to deliver medications orally (Musazzi et al., 2020). ODFs can rapidly disintegrate in the oral cavity without water which provides the unique advantage of ease the oral drug administration for patients who suffer from swallowing difficulties, primarily paediatric and geriatric or non-compliant patients (Gupta et al., 2020). ODFs can be single or multiple layers. The first prescription drug, ondansetron (Rapidfilm®), in the form of ODF, was approved in the EU in 2010 (Borges et al., 2015). Several prescription-only medications have been marketed subsequently, such as risperidone and fentanyl (Preis et al., 2015). The interest of ODFs is not only limited to mass production by pharmaceutical companies, but it has extended to small scale production of personalised medicine at the point of care to accommodate individual patient's clinical needs in dosing and drug combinations (Foo et al., 2018; Musazzi et al., 2018; Sandler and Preis, 2016).

A range of methods has been explored for centralised manufacturing ODFs in large batches with fix doses. Solvent casting is a common method discussed in the literature to prepare ODFs due to its simplicity (Hoffmann et al., 2011). Solvent casting is suitable for heat-sensitive APIs but suffering from the significant use of solvents and lengthy processes (long solvent evaporation). In addition, the casting method is not applicable for hydrolysis-sensitive APIs, and with limited drug load. Hot-melt extrusion is an alternative method to prepare ODFs (Morales and McConville, 2011). The polymer, APIs and other ingredients such as plasticisers are mixed inside an extruder with heating to form a homogenous mixture before being ejected through a die to form thin films (Karki et al., 2016). Hot-melt extrusion can improve the solubility of APIs with poor aqueous solubility by producing a solid dispersion, and no solvent is involved in the mixing process (Repka et al., 2005). However, disadvantages such as degradation of thermolabile APIs and limited polymer selections are associated with hot-melt extrusion (Low et al., 2013).

Additive manufacturing technologies have been explored as a class of new methods to produce ODFs, such as inkjet printing (Genina et al., 2013; Sandler et al., 2011; Wickström et al., 2015), semisolid extrusion 3D printing (Öblom et al., 2019), and fused deposition modelling 3D printing (Ehtezazi et al., 2018). These technologies provide flexibility in making ODFs with personalised drug doses to accommodate patient's needs and small-batch manufacturing at or close to the point of care, such as hospital pharmacies (Preis et al., 2015; Slavkova and

Breitkreutz, 2015; Trenfield et al., 2018). Inkjet printing is one of the printing technologies researched most extensively to produce ODFs with tailored doses (Scoutaris et al., 2016). Drop-on-demand inkjet printing technology can deposit picolitre droplets on the substrate with high precision and is the most discussed inkjet printing method in the literature for fabricating ODFs. In most literature, a commercial inkjet printer was used with a modified ink cartridge to dispense drug ink (Vuddanda et al., 2018). There are two methods reported in the literature to produce ODFs by inkjet printing. The most common method is to dispense drug-loaded ink on an edible supporting substrate, such as HPMC-based films (Planchette et al., 2016). The ink contains a drug with a viscosity modifier to facilitate the stable deposition of droplets onto the supporting substrate which is usually prepared by the solvent casting (Edinger et al., 2018b). The solvent in ink evaporates with time, leaving the drug molecules on the surface of the edible substrate. The printing is often repeated layer-by-layer to deposit enough APIs on the ODF. Printing APIs with unique patterns such as quick response (QR) codes containing information on patient details, medication, dosage, and batch details on HPMC film has also been attempted for quality assurance and tracking (Edinger et al., 2018a). A rare alternative approach is to directly print the ink containing polymer and drug onto the substrate to form ODFs (Cader et al., 2019; Sandler et al., 2011). The ink usually contains a film-forming polymer and a drug in a low concentration to maintain the viscosity within the printable range. Organic solvent or surfactants are often necessary to reduce the surface tension of the ink. For example, Cader et al. printed an ink containing polyvinylpyrrolidone, polysorbate 20, glycerol, thiamine hydrochloride in water on a PET substrate with appropriate droplets spacing to fuse all the droplets, resulting in a pore-less ODF (Cader et al., 2019).

However, inkjet printing has several significant limitations in fabricating ODFs. 1) Highly restricted low viscosity of the ink (below 20 mPa.s and surface tension in the range of 20-50 mN/m) to avoid nozzle blockage (Hutchings and Martin, 2013; Pardeike et al., 2011). 2) Low drug loading of inks, due to restricted viscosity, leading to large solvent content and long drying times. 3) Subsequently, thin layers of low drug content film were formed. For high dose formulations, multi-pass printing is usually required to deposit a sufficient amount of API on the ODFs. However, multi-pass printing results in a higher volume of solvent used and longer production time associated with longer printing time and solvent evaporation. 4) Interactions between drug ink and the edible supporting substrate increase the complexity of the ODFs printing. For example, Genina et al. studied the printing performance of rasagiline on different

123   substrates by inkjet printing and concluded that the selection of substrates could significantly

124   impact the uniformity of printed dosage (Genina et al., 2013).

125

126   In this study, we investigated whether a piezoelectric micro-dispensing (MD) system can

127   overcome some of the challenges faced by inkjet printing for ODF fabrication with

128   personalised dose adjustment capability. MD enables precisely dispensing a range of low and

129   high viscosity (up to 2,000,000 mPa.s) materials to produce droplets, beads, and lines at high

130   speed (Vermes GmbH, 2020). There are two main types of MD printhead, the piezoelectric

131   driven printhead and solenoid actuated printhead (Wong et al., 2009). The piezoelectric

132   actuated printhead contains a piezoelectric tappet rod in the dispensing chamber to control

133   liquid flow by moving upwards and downwards in response to electrical signals. The solenoid-

134   actuated printhead relies on the magnetic field change to control the opening of the dispensing

135   valve for liquid dispensing. Both systems require pneumatic control to push the liquid out of

136   the orifice to form droplets and excel at different fabrication tasks (Wong et al., 2009). The

137   main advantage of using MD for ODF fabrication is the capability to accurately dispense a low

138   volume of viscous liquid without using an edible supporting substrate. Although to the best of

139   our knowledge MD has not been reported for ODFs fabrication, it has been explored to

140   fabricate tailored dose medications. Bonhoeffer et al. used a piezoelectric micro-dispensing

141   system to dispense nanosuspension to placebo drug carriers (i.e. excipient filled capsules or

142   placebo tablets) as a new concept to produce personalised solid dosage forms (Bonhoeffer et

143   al., 2018).

144

145   This study reports the first use of MD as a single-step method to prepare personalised ODFs

146   without edible supporting substrate. The aim is to demonstrate the fabrication of personalised

147   ODFs by a MD system and understand the droplet fusions and film-forming properties as well

148   as their impact on the disintegration behaviour of the printed ODFs. By using the preformulated

149   polymer-drug ink delivered to the point of care, such as hospital pharmacies, on-demand

150   manufacturing of ODFs could be done by MD systems. The preformulated ink contains

151   hydroxypropyl methylcellulose (HPMC) as the model polymer and paracetamol as the model

152   drug. HPMC, with the particular grade of Pharmacoat 606, is selected because of its excellent

153   film-forming, rapid hydration and disintegration properties. Paracetamol is used as the model

154   drug to demonstrate the dose adjustment capability of ODFs prepared by MD printing

155   according to patients' clinical needs. A printing sequence was designed to produce ODFs with

156   various doses by using an 'universal' ink (an ink with a fixed model drug concentration), but

157 only changing the film dimension. The solvent casting method was used as a control method

158 to prepare ODFs for comparing the physical and mechanical properties, uniformity of drug

159 content and disintegration of the ODFs. The proof-of-concept results of dose adjustment

160 capability of MD printing indicates that the technology has the potential for not only point of

161 care ODFs production in small batches, but also other liquid dispensing and coating

162 applications for personalised medicine and device fabrications.

163

164 **2. Materials and methods**

165 **2.1. Materials**

166 Hydroxypropyl methylcellulose (HPMC) (commercial name as Pharmacoat 606) was kindly

167 donated by Shin-Etsu (Niigata, Japan) and used as the film-forming polymer to fabricate the

168 ODFs. Paracetamol and phosphate buffer saline (PBS) tablet pH 7.4 were purchased from

169 Sigma-Aldrich (Gillingham, UK). Polyethylene terephthalate (PET) plastic film (KF26066)

170 was purchased from Q-connect (Sheffield, UK) and used as the substrate for printing and

171 casting ODFs. Milli-Q (Millipore, Merck, USA) ultra-pure water was used as the solvent.

172 Listerine PocketPaks® breath strips (a pullulan-based oral film) were purchased from Johnson

173 & Johnson (New Brunswick, USA). All materials were used without further processing. The

174 model of the MD system used in this study is a Nanojet Piezo Valve NJ-K-4020 with an inner

175 nozzle diameter of 200 μm. The MD system was purchased from Microdrop Technologies

176 GmbH (Norderstedt, Germany).

177

178 **2.2. Preparation of placebo and polymer-drug inks**

179 Three concentrations of HPMC solutions (5%, 10% and 15% w/v) were prepared as the placebo

180 ink to characterise the MD system. The polymer was dissolved in water with stirring at 50 ºC

181 using a magnetic stirring hot plate until all powder dissolved and allowed to degas overnight

182 at ambient condition. The polymer-drug ink (HPMC 15% w/v, paracetamol 1.4% w/v) was

183 prepared by dissolving all the dry ingredients into the water and followed the same procedure

184 as the placebo ink. All resulting solutions were filtered by a glass fibre syringe filter with 5 μm

185 pore size (OU-12915-33, Cole-Parmer GmbH, Wertheim, Germany) and allowed to settle

186 down before printing.

187

188 **2.3. MD printing system setup**

189 The components of the MD system built in-house are shown in **Fig. 1**. The system consists of

190 an air compressor to pressurise the ink reservoir, a computer to control the movement of the

6

191 motorised x-y translation stage (MTS-25, Thorlabs, USA) and design the printing sequence, a

192 control unit to tune the dispensing parameters and to control supplied pressure to the liquid

193 reservoir, a liquid reservoir and the MD printhead attached to a manual z-translation stage
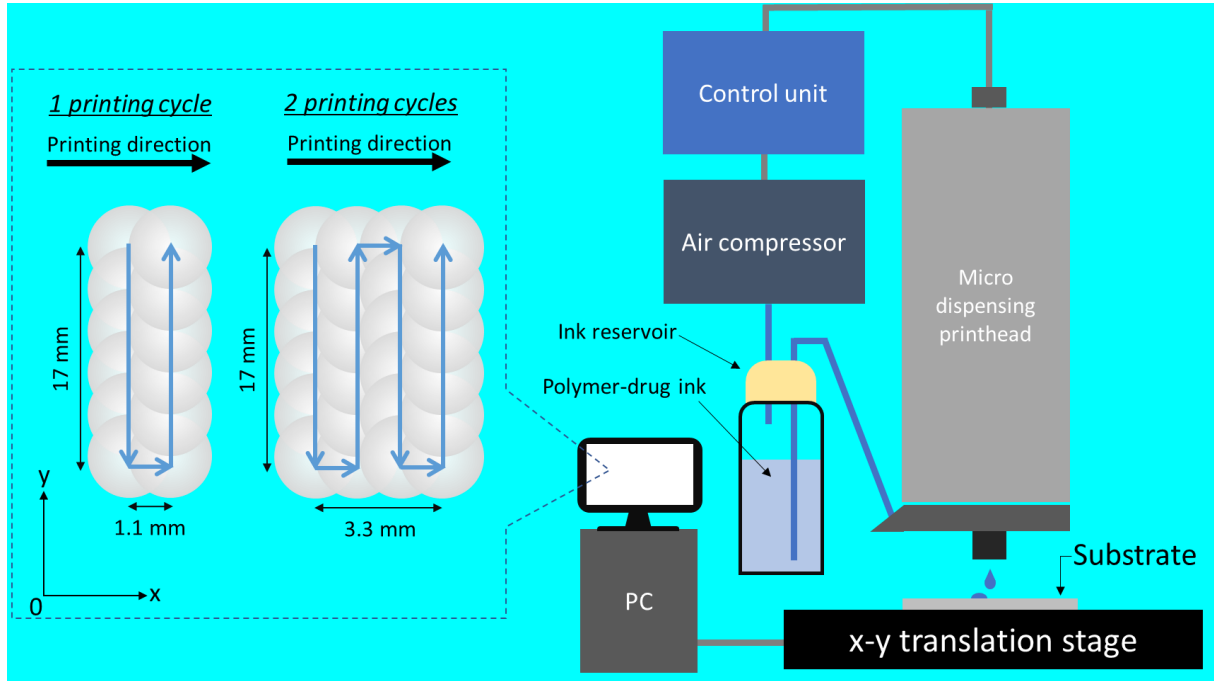
194 (PT1B, Thorlabs, USA).

195

Fig. 1. *Schematic diagram of the MD system built in-house to print ODFs on-demand*

(droplets and components are not to scale) with exemplar printpath designs with 1 and 2

printing cycles.

199

Fig. 2 illustrates the dispensing mechanism of the piezoelectric MD printhead and the

corresponding dispensing parameter. The applied voltage activates the movement of the tappet

rod to break the liquid stream into droplets. The opening height indicates the tappet rod's

relative distance from the nozzle, from 100 % as fully lifted and 0 % as no movement. The

opening time is the time interval when the valve is fully open. The rising time and falling time

are the time interval when the tappet rod is moving up and down, respectively. Delay time

defines the idle time between each complete dispensing cycle. The detailed printing parameter

optimisation is discussed in the Results section. The optimized printing sequence was designed

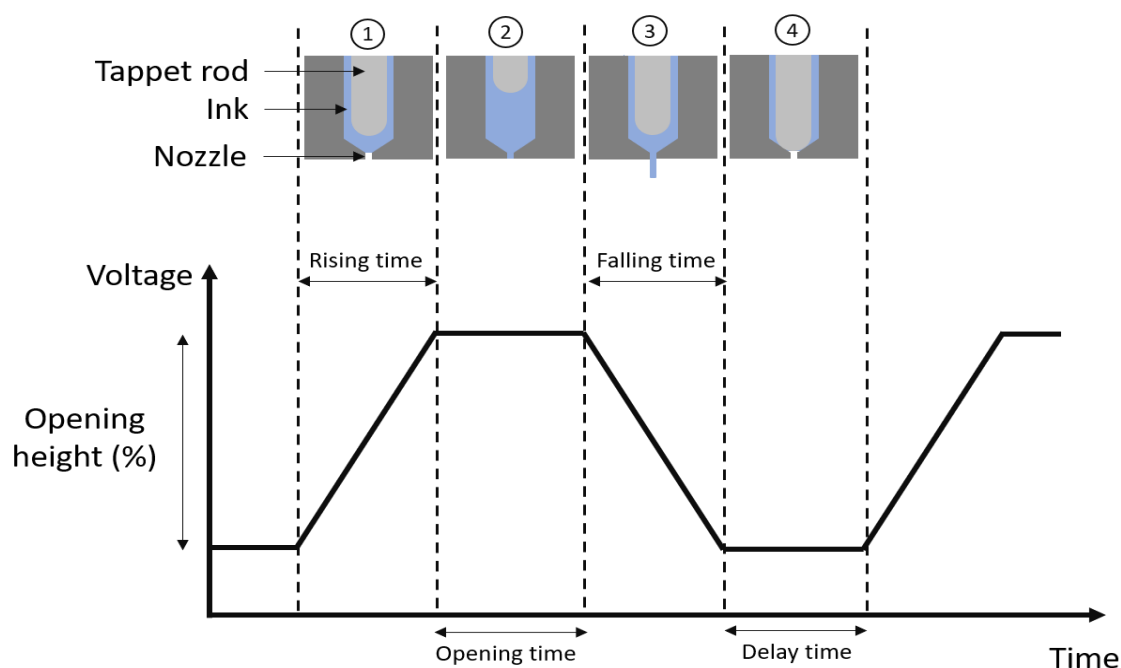using the Kinesis software (version 1.14.15, Thorlabs, USA).

Fig. 2. The waveform of driving voltage for dispensing and the corresponding location of the

tappet rod.

2.4. Physical properties of placebo and polymer-drug inks

2.4.1. **Viscosity**. The viscosity of polymer-drug ink was measured by a Discovery HR-2 rheometer (TA instrument, Delaware, USA) equipped with a 40 mm, 2° cone plate geometry. The method was set to be a flow ramp procedure from 0.1 to 60 s^{-1} at 25 °C. The results were fitted to the Newtonian model to obtain the dynamic viscosity. Measurement was done in triplicate to calculate the average viscosity.

2.4.2. Density The density of the solutions was measured by a density meter DMA 4500M (Anton Paar GmbH, Graz, Austria) equipped with an oscillating U-tube. The measurement was done by injecting 1 ml of the sample into the system at 25 °C. The measurement was done in triplicate to obtain the average density.

2.5. Effects of MD printing parameters on the accuracy of dosing volume

The placebo inks were used to investigate the critical operational parameters of the MD printing that can affect the accuracy of the volume dispensed. The importance of understanding this is that the accuracy of the dispensing volume is directly linked to the accuracy of the drug dispensed into the ODFs. The one-factor-at-time approach was adopted. The rising time and falling time were set to the minimum value for ease of characterisation. The gravimetric method

was adopted from Bonhoeffer et al. to measure the change of dispensing volume against different dispensing parameters (Bonhoeffer et al., 2017). The dispensing volumes were measured when one of the four key operational parameters were altered, and the rest were kept constant. The investigated parameters include pressure, opening height, opening time and delay time. Within each experiment set, ten drops of the placebo ink were dispensed into a pre-weight glass vial containing dodecane as barrier liquid (to prevent evaporation) and the weight difference before and after dispensing was measured. The dispensing volume was calculated using the density equation, $\rho = m/v$, where ρ is the density, m is the mass and v is the volume. For each set of parameter changes, three independent sets of ten drops dispensing were performed and measured to examine the reproductivity of the tests. A light microscope FDSC196 (Linkam Scientific, Tadworth, UK) was used to observe the change of droplet morphology with different dispensing parameters.

2.6. Fabrication of ODFs

2.6.1. Cast ODFs: The cast ODF was prepared by casting 10 ml of the polymer-drug ink stated above onto the PET substrate by an adjustable film applicator 1117 / 100 mm (Sheen Instruments, Herefordshire, UK) set at 550 µm gap height. The cast ODF was dried in an oven set at 30 °C for approximately 2 hours. The resulting film was cut into square films with 18 mm x 18 mm dimensions using a craft puncher before storing in a desiccator for further measurements.

2.6.2. MD printed ODFs: The optimised printing parameters were used to print ODFs. One printing cycle is defined as shown in **Fig. 1**. Once the dispensing started, the translation stage moved in the y-direction from the pre-set coordinate towards the zero point, followed by the movement to the x-direction. The translation stage moved back to the original y coordinate when the movement along the x-axis was completed. The print area of ODFs was increased by repeating the printing cycle in the x-direction. The ODFs were formed by depositing a specific number of droplets as one printing cycle onto the PET substrate using the optimised dispensing parameters reported in **Table 1**. It is worth noting that the frequency of droplet dispensing is not specified here. It is controlled by combining a range of operational parameters, including the raising, the falling, the opening and the delay time. These are discussed in the Result section. The dimension of ODFs was increased by repeating the printing cycles (1, 2, 4, 6 and 8) to expand the print area in the x-direction. The printing time for the 1, 2, 4, 6, and 8 cycles

264 are 16, 32, 65, 98 and 131 seconds, respectively. The printed ODFs were subsequently dried in

265 a 30 °C oven for 2 hours before being stored in a desiccator.

266

267 **2.7. Physical characterisation of cast and printed ODFs**

268 **2.7.1. Thickness:** The thickness of 18 mm x 18 mm cast ODFs, printed ODFs and Listerine

269 PocketPaks® films were measured by an electronic thickness gauge ET-3 (Rehder-dev,

270 Greenville, USA). The measurement was performed at four corners and the centre of the film,

271 except printed ODFs with one and two printing cycles due to the narrow dimension in width,

272 three measurements at centre, top and bottom of the film were taken instead. Five samples of

273 each type of film were measured and the average thickness was calculated.

274

275 **2.7.2. Weight:** The weight of printed ODFs with different printing cycles and cast ODFs were

276 measured by the analytical balance XS205DU (Mettler Toledo, Leicester, UK) after the film

277 was stored in the desiccator for 24 hours. The average weight was calculated by five samples

278 from each type of film.

279

280 **2.7.3. Surface morphology:** The surface morphology of the printed and cast films was

281 characterised by Scanning Electron Microscope (SEM). Film samples were cut and attached to

282 a sample holder with carbon adhesive tape and sputter-coated with gold for 30 seconds and 2.2

283 kV at 55 mm and $5x10^{-2}$ mbar (Quorum Technologies, Lewes, UK). Images of cross-section

284 and surface of printed and cast films were captured using a Gemini 300 series SEM (Zeiss,

285 Germany).

286

287 **2.7.4. Mechanical properties of ODFs**

288 Four samples of the 18 mm x 18 mm MD printed ODFs and cast ODFs were subjected to

289 mechanical testing using a Texture Analyser TA-XTplus (Stable Micro Systems, Godalming,

290 UK) to determine the tensile strength and elongation at break. Listerine PocketPaks® films

291 were used as the guide of film handling by comparison with the cast and printed films. The

292 films were fixed between two clamps with a 1 cm gap using tensile grips A/TG (Stable Micro

293 Systems, Godalming, UK). The clamps moved away from each other with 50 mm/min velocity

294 until the film was torn. Tensile strength (N/mm^2) is defined as the maximum force required to

295 break the film and calculated by Eq. (1).

296 $$Tensile\ strength = \frac{force\ at\ break}{cross-sectional\ area\ of\ films} \quad \dots Eq.\ (1)$$

297

Elongation at break (%) is defined as the ratio of length increased after fracture to the original length of the film as shown in the Eq. (2).

$$Elongation\ at\ break = \frac{increased\ lenght\ at\ break}{original\ length}\ x\ 100\ \ \text{...Eq. (2)}$$

301

2.8. Differential Scanning Calorimetry (DSC)

Thermal measurement was conducted by using differential scanning calorimeter DSC 2500 (TA instrument, USA). All samples and raw materials were separately crimped in an aluminium pan. Paracetamol and HPMC were subject to the standard heat-cool-heat cycle at 20 °C/min heating and cooling rate. The film samples were cut to fit the aluminium pan and heated to 220 °C at 20 °C/min. All measurements were conducted with nitrogen as the purge gas with a 50 ml/min flow rate. The analysis was performed by TRIOS software (TA instrument, USA).

310

2.9. Thermogravimetric Analysis (TGA) for moisture content

A thermogravimetric analyser, TGA 5500 (TA instrument, USA), was used to evaluate the moisture content in the ODFs. Three samples (approximately 2.5 - 6 mg) from MD printed films with different printing cycles and cast film were measured. The films were placed on platinum pans and heated from 25 °C to 300 °C at a rate of 10 °C/min under a continuous flow of nitrogen (50 ml/min). The weight change between 25 °C to 100 °C is considered the loss of moisture from the film and analysed using TRIOS software (TA Instruments, USA).

318

2.10. Attenuated total reflection Fourier transform infrared (ATR-FTIR) spectroscopy

The distribution of paracetamol at different areas of the MD printed with eight printing cycles and the cast films and any potential drug-polymer interactions were studied using the ATR-FTIR spectrometer Vertex 70 (Bruker Optics Ltd, Coventry, UK) equipped with a golden Gate Attenuate Total Reflectance accessory (Space Ltd, Orpington, UK). Three random locations on each film were selected for measurement. The measurement was performed from the wavenumber range of 500 – 4000 cm^{-1} at a resolution of 2 cm^{-1} and 32 scans. The results were analysed using the OPUS software version 7.8 (Bruker Optics Ltd, Coventry, UK).

327

2.11. Drug content measurements of ODFs

329   The cast ODFs and MD printed ODFs were dissolved individually in 5 ml of PBS pH 7.4 and

330   diluted accordingly to be quantified by the UV-Vis spectroscopy Lambda 35 (PerkinElmer,

331   Massachusetts, USA). A calibration curve of paracetamol in PBS was built by measuring the

332   concentration ranged from 1.5 µg/ml to 15 µg/ml at the λ_{max} of 244 nm. Five samples from

333   printed films and cast films were used to calculate the average value.

334

335   **2.12. Disintegration test of ODFs**

336   A modified petri dish method was adopted to evaluate the disintegration time of MD printed

337   and cast ODFs (Alhayali et al., 2019). A watch glass with a 10 cm diameter containing 2 ml

338   PBS pH 7.4 was equilibrated in a shaking incubator (KS 3000 I control, IKA, Germany) set at

339   60 rpm and 37 ± 0.5 °C. The films were laid on PBS and recorded the time when the film

340   started to disintegrate (Chonkar et al., 2016). The measurement was done in triplicate for all

341   types of films.

342

343   **2.13. Statistical analysis**

344   The basic calculation was performed by Microsoft Excel® (Microsoft Office 365). The data

345   analysis was performed using SPSS statistical program (SPSS 25, IBM, New York, USA).

346   Analysis of variance (ANOVA) and Tukey test were used to compare the thickness of ODFs

347   at different locations. A statistical significance is considered when the p-value is lower than

348   0.05.

349

350   **3. Results and discussion**

351   **3.1. Effects of MD printing parameters on the accuracy of dosing volume**

352   The placebo HPMC ink was used to determine the effect of dispensing parameters on

353   dispensing volume. Briefly, the dispensing volume is influenced by the opening time (ms),

354   applied pressure (kPa) and opening height (%), as illustrated in **Fig. 3**. The applied pressure

355   must be sufficiently high to ensure the liquid has enough velocity to leave the nozzle and travel

356   to the substrate. Low applied pressure does not dispense the ink because of the accumulation

357   of fluid at the nozzle. Higher applied pressure increases the dispensing volume, but the effect

358   on dispensing volume was less than the effect of than the opening time. As seen in **Fig. 3A**, for

359   all concentrations of HPMC in the ink the volume of the placebo ink dispensed was linearly

360   proportional to the applied pressure. There is no linear correlation between dispensing volume

361   and opening height (**Fig. 3B**). Air bubbles were observed in the droplets when the opening

362   height was set to 100%, as shown in **Fig. 4**. Such an issue was mitigated by reducing the

363   opening height beyond 50%, but the dispensing volume decreased substantially at this level.

364   The opening time is the most critical parameter to control dispensing volume. As seen in **Fig.**

365   **3C**, the opening time is highly linearly correlated with the dispensing volume for all three

366   placebo inks tested. More importantly, compared to **Fig. 3A**, the sensitivity of the opening time

367   to adjust the dispensing volume is much greater than the pressure. By changing the opening

368   time from 10 ms to 200 ms, the dispensed volume of 5% HPMC ink can be changed from less

369   than 20 µl to nearly 600 µl. The test range of delay time has a minimal impact on the dispensing

370   volume as shown in **Fig. 3D**. The differences in viscosity of placebo inks accounted for the

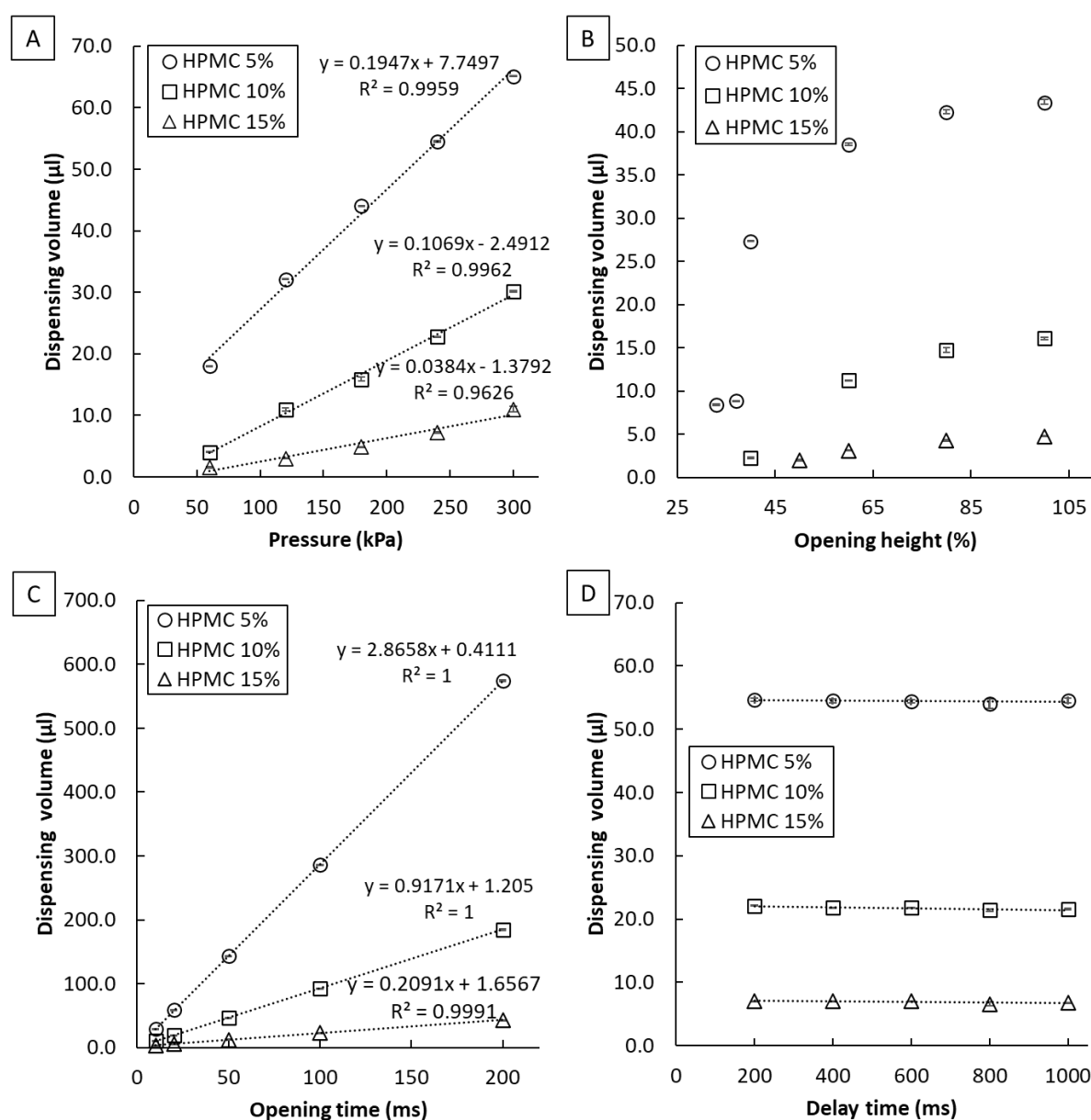371   change in dispensing volume.

372

373

Fig. 3. *The correlations between dispensing volume of the placebo HPMC ink and (A)*

375 *pressure; (B) opening height; (C) opening time and (D) delay time. For each graph, only the*

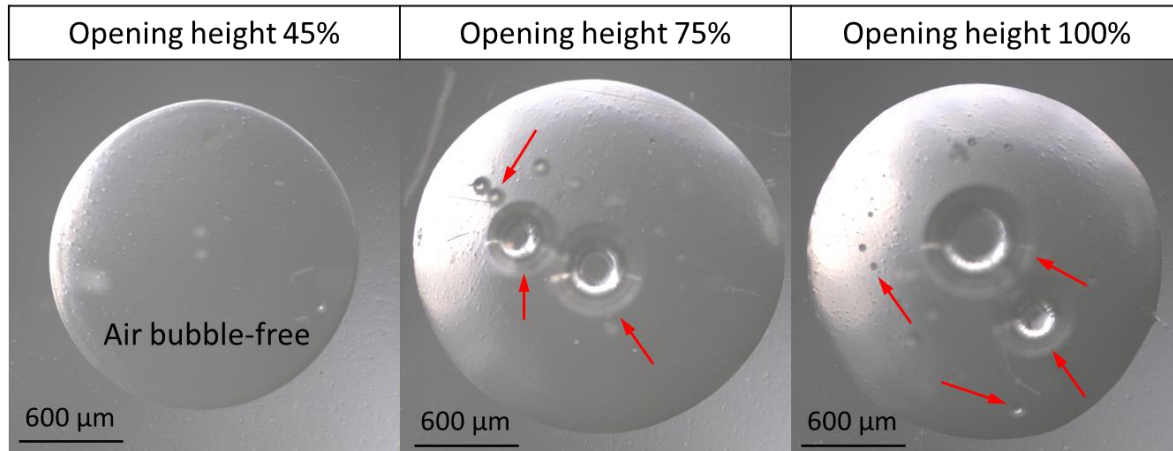376 *defined parameter was changed. The rest of the operational parameters remained constant.*

377

378 **Fig. 4.** *Example microscopic images of the droplet of the placebo HPMC ink containing air*

379 *bubbles (highlighted by arrows) dispensed at different opening heights.*

380

381 3.2. MD printing parameter optimisation for drug loaded ODF fabrication

382 Following the investigation into the effects of individual printing parameters on the dispensing

383 volume, the printing parameter optimisation using the polymer-drug ink (HPMC 15% w/v,

384 paracetamol 1.4% w/v) was performed. The nozzle-substrate distance was set as low as

385 possible to expand the operational range for other dispensing parameters (Bonhoeffer et al.,

386 2017). The rising time and falling time were set to the minimum value for the ease of

387 optimisation. The opening height was first adjusted to produce droplets free of bubbles to

388 ensure bubble- and defect-free films. The pressure was adjusted to ensure the droplet had

389 sufficient velocity to leave the nozzle without splashing when it landed onto the substrate. Once

390 these were optimised, the opening time was optimised to allow the dispensing of droplets with

391 diameters of 1.65 mm so that the overlapping of droplets forms a straight line with 18 mm in

392 length. Finally, the delay time was adjusted according to the movement speed of the x-y

393 translation stage (2.4 mm/s) to control the degree of overlapping of droplets. The optimised

394 printing parameters adopted to print ODFs are shown in **Table 1**.

395

396 **Table 1**. *Optimised printing parameters for printing drug loaded ODFs by the MD system*

Pressure (kPa)	295
Opening height (%)	45

Opening time (ms)	14
Rising time (ms)	0.5
Falling time (ms)	0.3
Nozzle substrate distance (mm)	3
Delay time (ms)	350

397

3.3. Ink characterisation

399 The main advantage of MD in comparison to inkjet printing is the capability to dispense viscous

400 ink. The viscosity of the ink has a direct impact on droplet spreading on the substrate and drug

401 distribution. A highly viscous solution can reduce its spreading on the PET substrate and thus

402 achieve a higher quantity of drug per area. The high ink viscosity also enables single-pass

403 printing to fabricate ODFs with sufficient thickness and drug load. This is a major challenge

404 for direct inkjet printing of ODFs. The measured dynamic viscosity of 15% w/v HPMC placebo

405 ink was 813.92 ± 1.72 mPa.s. The dynamic viscosity of the polymer-drug (15% w/v HPMC

406 and 1.4% w/v paracetamol) ink was 818.32 ± 4.45 mPa.s as shown in **Table 2**. The polymer-

407 drug ink behaved as a Newtonian fluid since the shear stress and shear rate showed a linear

408 relationship. There is no statistical difference between the placebo and polymer-drug ink ($p =

409 0.223 > 0.05$).

410

411 **Table 2.** *Physical properties of placebo and polymer-drug inks*

Formula	Viscosity (mPa.s)	Density (g/ml)
HPMC 5% w/v	32.58 ± 1.65	1.009 ± 0.001
HPMC 10% w/v	202.18 ± 2.62	1.020 ± 0.001
HPMC 15% w/v	813.92 ± 1.72	1.031 ± 0.001
HPMC 15% + paracetamol 1.4% w/v	818.32 ± 4.45	1.031 ± 0.010

412

3.4. Thickness and surface morphology of drug loaded ODFs

414 **Fig. 5A** demonstrates the locations of measurements for the thickness of ODFs. The thickness

415 of 18 mm x 18 mm drug loaded ODFs prepared by solvent casting, MD printing (with eight

416 printing cycles) and Listerine PocketPak® films is shown in **Fig. 5B**. The average (taking into

417 consideration of corners and centres of the films) thickness of cast films and MD printed films

418 were 60.12 ± 1.67 µm and 51.24 ± 8.8 µm, respectively. The thickness of Listerine PocketPak®

419 films is 45.64 ± 1.04 µm. In terms of the evenness of the thickness across the films, the cast

420   films and Listerine PocketPak[®] films showed even thickness throughout the film ($p = 0.932 >$
421   0.05 and $p = 0.508 > 0.05$, respectively); whereas the MD printed films showed uniform
422   thickness at the corners ($p = 1 > 0.05$) with an elevated centre ($p = 0.0001 < 0.05$) (**Fig. 5B**).
423   The marketed product, Listerine PocketPak[®] films, is used as the benchmark to assess the film
424   quality, since it shows high consistency in the thickness of the entire film. The results on this
425   film obtained by us agree with other reported results (Preis et al., 2014). The higher evenness
426   of the film thickness of the cast film is because the cast films tested were cut from the centre
427   of a large parent film. The cast parent films had significantly thinner edges than the centres,
428   thus only the central areas were used. For the MD printed films, the thicknesses of the edges
429   and centres are the true representation of the properties of the film directly after manufacturing.
430   So the data quoted here represents the properties of the films they would be used in practice
431   and are not accurate representations of the intrinsic material properties but are those of whole
432   films.
433
434   It was observed that the drying of the MD printed drug loaded ODFs originated from the edge
435   of the film and emerged slowly towards the centre. The possible cause of the higher thickness
436   of the centre of the MD printed ODFs in comparison to the corners may be explained by the
437   lateral spreading of the wet film, as illustrated in **Fig. 5C**. As defined by the printpath design,
438   there is a degree of overlap between individual droplets. After deposition, this leads to rapid
439   coalescence or fusion of adjacent droplets to form the liquid 'pool' and cause opposing flow in
440   the centre. However, at the edges, there is mainly lateral spreading of the droplets deposited at
441   the outer edge leading to formation of a thinner layer of liquid than the centre prior to
442   solidification via drying. The large parent film prepared by the casting method also exhibited
443   lateral spreading, resulting in nonuniform thickness with thinner edges and a thicker centre.
444   However, the cast films used as the controls were cut from the centre of the parent film using
445   an 18 mm x 18 mm craft punch, thus exhibited good consistency of the thickness of the corners
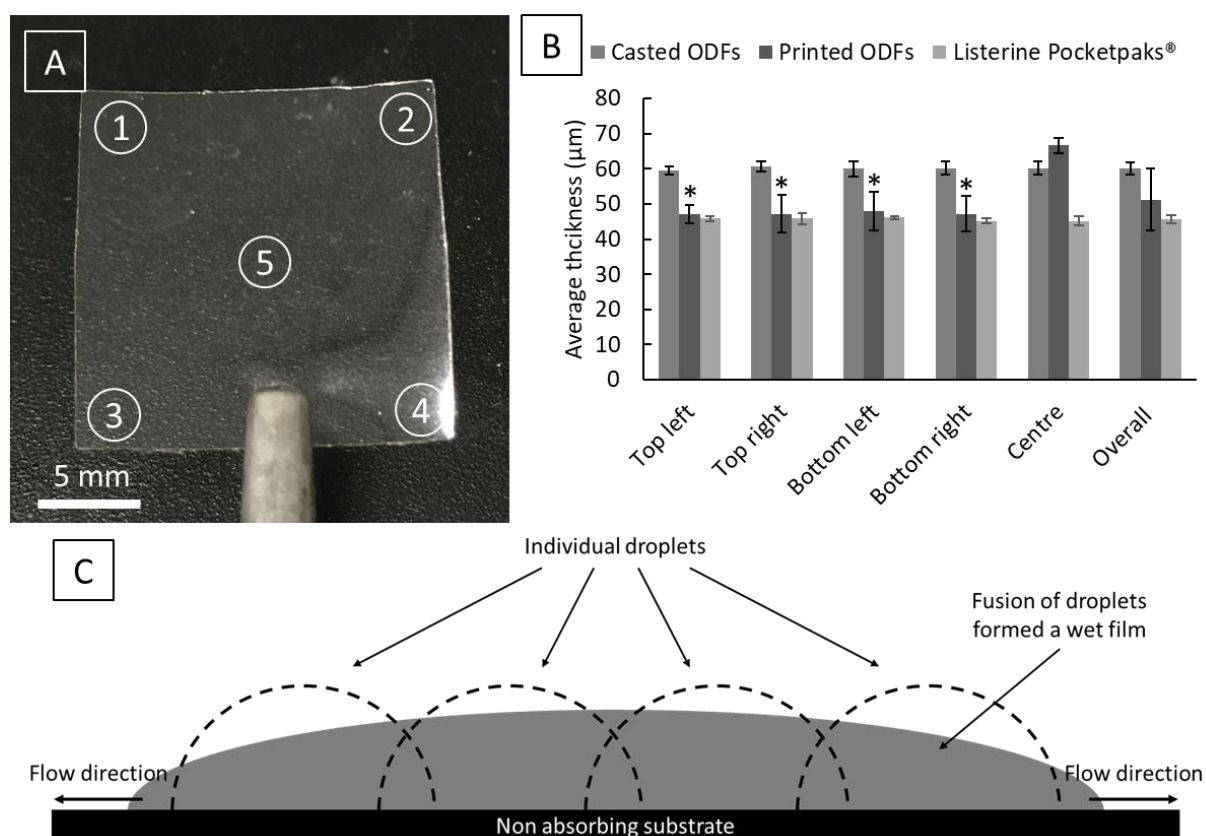446   and the centres.
447

Fig. 5. *(A) An exemplar drug loaded ODF prepared by casting method to show the location of measurement; (B) the thickness of 18 mm x 18 mm cast, MD printed drug loaded ODFs (with eight cycles) and Listerine PocketPak® films at different locations. Asterisks refer to a statistically significant difference (p = 0.0001 < 0.05) with the thickness at the centre; (C) graphic illustration of the drying and ODF film formation processes of the partially overlapped droplets deposited by MD.*

3.5. Surface morphology of MD printed drug loaded films

The texture of drug loaded ODFs can affect patients' acceptance to some extent. The film should show a homogenous surface or colour to demonstrate its quality (Wasilewska and Winnicka, 2019). As discussed earlier, ODFs prepared by inkjet printing often require the printing of drug containing inks onto a pre-prepared edible substrate film. This poses the risk of substrate malformation because of the printing process (Scoutaris et al., 2016). It is often attributed to the high proportion of solvent used in inkjet printing ink to control viscosity. The solvent can solubilise the substrate film upon contact, leading to an uneven substrate surface after multi-pass printing. The MD uses a single-pass printing approach to fabricate ODFs to reduce the risk of poor surface texture associated with overprints. The surface properties of cast and MD printed drug loaded ODFs are shown in **Fig. 6**. The MD printed ODFs demonstrated

17

467   a smooth surface (**Fig. 6A - D**), indicating the overlapping of droplets were sufficient to allow

468   the complete fusion of adjacent droplets to form a homogenous film. The cross-sectional

469   images of printed ODFs show homogeneous distribution of materials. Similar surface

470   morphology was also observed from the cast film (**Fig. 6E - H**). A layered appearance is

471   observed in some of the cross-sectional images of the MD printed ODFs, but not in others.

472   Thus, we believe the appearance of the layering is due to the artefacts caused during the cutting
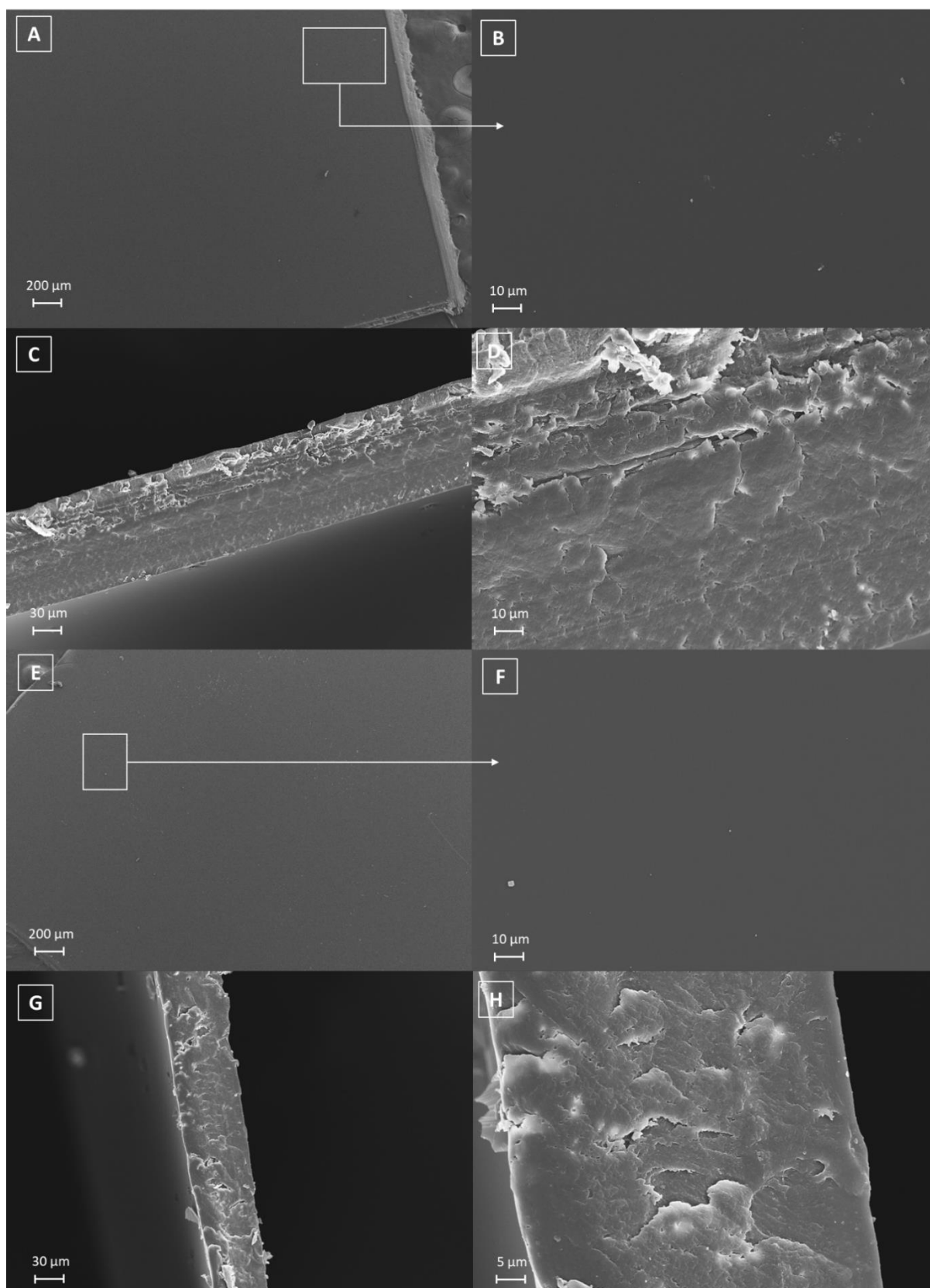
473   process of the films.

474

475

Fig. 6. *Representative SEM images of the drug loaded ODFs prepared by MD printed with low (A,C, E, G) and high (B, D, F, H) magnifications (with 8 printing cycles) (A & B: surface, C & D: cross-section) and by casting (E & F: surface, G & H: cross-section).*

3.6. Physicochemical characterisation of the drug loaded ODFs

Table 3. shows the measured physicochemical properties of MD printed and cast ODFs. A range of printing cycles, between one to eight, were used to produce the films and investigate the correlation between the number of printing cycle and mechanical properties (section 3.7), film weight, film thickness and drug content (section 3.8), and disintegration behaviour (section 3.9). All printed films were set to have a fixed length of 18 mm and the film width and the overall film area were expanded by increasing the number of printing cycles. It is worth noting that although the width of the film in increasing in a linear fashion with the number of the printing cycles, the films with one printing cycle proportionally are wider in width (averagly 2.7 mm) than other films. The film thickness of the films printed using two to eight printing cycles are relatively consistent. The film thickness of the film printed with one printing cycle is significantly thinner than the others. It is noted that the width of the films printed with one printing cycle is averagly 2.7 mm. This correlates well with the proportionally wider (in width) of the film prinited with 1 printing cycle than others. Eight printing cycles provide a film with a dimension of 18 mm x 18 mm which is comparable to the cast films, thus used for further mechanical testing. The data demonstrated that the dimension and drug dose of the MD printed films is freely adjustable by altering the number of printing cycles.

Table 3. Physical characterisation, concentration and disintegration time of drug loaded ODFs prepared by MD printing and casting (n=5)

Printing cycle(s)	1	2	4	6	8	Cast
Print time(s)	16	32	65	98	131	-
Film dimension: **Width (mm) x** **Length (mm)**	2.7 x 18.0	4.6 x 18.0	9.4 x 18.0	13.6 x 18.0	18.0 x 18.0	18.0 x 18.0
Film weight ± SD (mg)	2.98 ± 0.34	5.88 ± 0.35	10.30 ± 0.34	14.46 ± 0.21	18.86 ± 0.08	23.34 ± 0.55
Film thickness (μm)	40 ± 2	49 ± 6	49 ± 10	50 ± 7	51 ± 9	60 ± 2
Paracetamol content ± SD (μg)	235.17 ± 24.25	453.22 ± 28.88	775.78 ± 53.19	1115.90 ± 16.46	1372.20 ± 16.27	1779.74 ± 46.56
Moisture content (%) ± SD	2.82 ± 0.79	2.46 ± 0.40	2.63 ± 0.23	3.16 ± 0.39	2.20 ± 0.74	2.93 ± 0.07

Disintegration time ± SD (s)	19.0 ± 4.0	28.7 ± 5.5	26.0 ± 5.3	30.7 ± 3.1	29.0 ± 3.6	30.0 ± 3.6

501

502   TGA was used to determine the moisture content of printed and cast films, as shown in **Table**

503   **3**. The MD printed films show a range of moisture content from 3.16 to 2.2%, while there is

504   2.93% moisture in the cast films. The moisture content of ODFs could impact the crystal state

505   of the API and the mechanical properties of ODFs. The low moisture content that remained in

506   the ODFs was likely due to the hygroscopic nature of HPMC. A small quantity of moisture

507   also can act as a plasticiser and provide flexibility to the film. Since the ODFs prepared by MD

508   is on-demand and expected to be administrated within a short time, the influence of moisture

509   on the quantity of ODFs is less concerned.

510

511   The physical state of the model drug in the drug loaded ODFs was characterised using a range

512   of analytical methods. The DSC results shown in **Fig. 7** shows a sharp endothermic melting

513   peak of crystalline paracetamol powder at 171.9 °C and a glass transition temperature (T_g) of

514   pure HPMC at 133.3 °C. The lack of paracetamol melting from the DSC results of the MD

515   printed and cast ODFs indicated paracetamol was in amorphous state. As the T_g of amorphous

516   paracetamol is 23 °C (Sibik et al., 2014), the drug would plasticise the polymer and the T_g of

517   the HPMC-paracetamol dispersion ODF is expected to be below 133 °C. The board peak at

518   about 90 °C from the thermogram of printed and cast ODFs reflects the presence of moisture

519   in the ODFs. The moisture contents could further reduce the T_g of the ODFs to a temperature

520   range that overlaps with the broad moisture loss peak. It may explain the absence of the T_g of

521   the ODF.

522

523   The ATR-FTIR data of the drug loaded MD printed with eight printing cycles and cast films,

524   the reference raw materials and their physical mixture are shown in **Fig. 7B**. The characteristic

525   peaks of Form I paracetamol have been well characterised by other literature (Al-Zoubi et al.,

526   2002; Wang et al., 2002) and the obtained IR spectrum of paracetamol matches the reported

527   data. The pure HPMC shows characteristic peaks at 3449 cm^{-1} (O-H stretching), 2903 cm^{-1} (C-

528   H stretching), 1453 cm^{-1}(C-H scissoring), 1374 cm^{-1}(O-H bending) and 1053 cm^{-1}(C-O

529   stretching). The spectrum of the physical mixture is a simple sum of the spectra of crystalline

530   paracetamol and HPMC. The broadened characteristic crystalline paracetamol peaks at 3321

531   cm^{-1} (N-H stretching) and 3108 cm^{-1} (O-H stretching) in the spectra of cast and MD printed

532   films indicate that paracetamol is in its amorphous state and consistent with molecular

533   dispersion (Qi et al., 2008). The shift of peak from 1505 cm^{-1} (aromatic ring mode) to 1514

534   cm^{-1} in cast film and MD printed film has been reported previously and is consistent with the

535   molecular dispersion of the drug in the polymer (Wang et al., 2002). No apparent shifts of

536   HPMC characteristic peaks are observed; thus, minimal drug-polymer interaction is indicated.

537   Three random locations on the cast and MD printed ODFs were examined by ATR-FTIR to

538   access the evenness of drug distribution. The relative intensities of the peaks at 1514 cm^{-1} were

539   used as the signature peaks of the concentration of paracetamol contents. There is no significant

540   difference observed in the spectra of different locations within the films (data not shown),

541   indicating paracetamol are evenly distributed in the printed films with eight printing cycles.
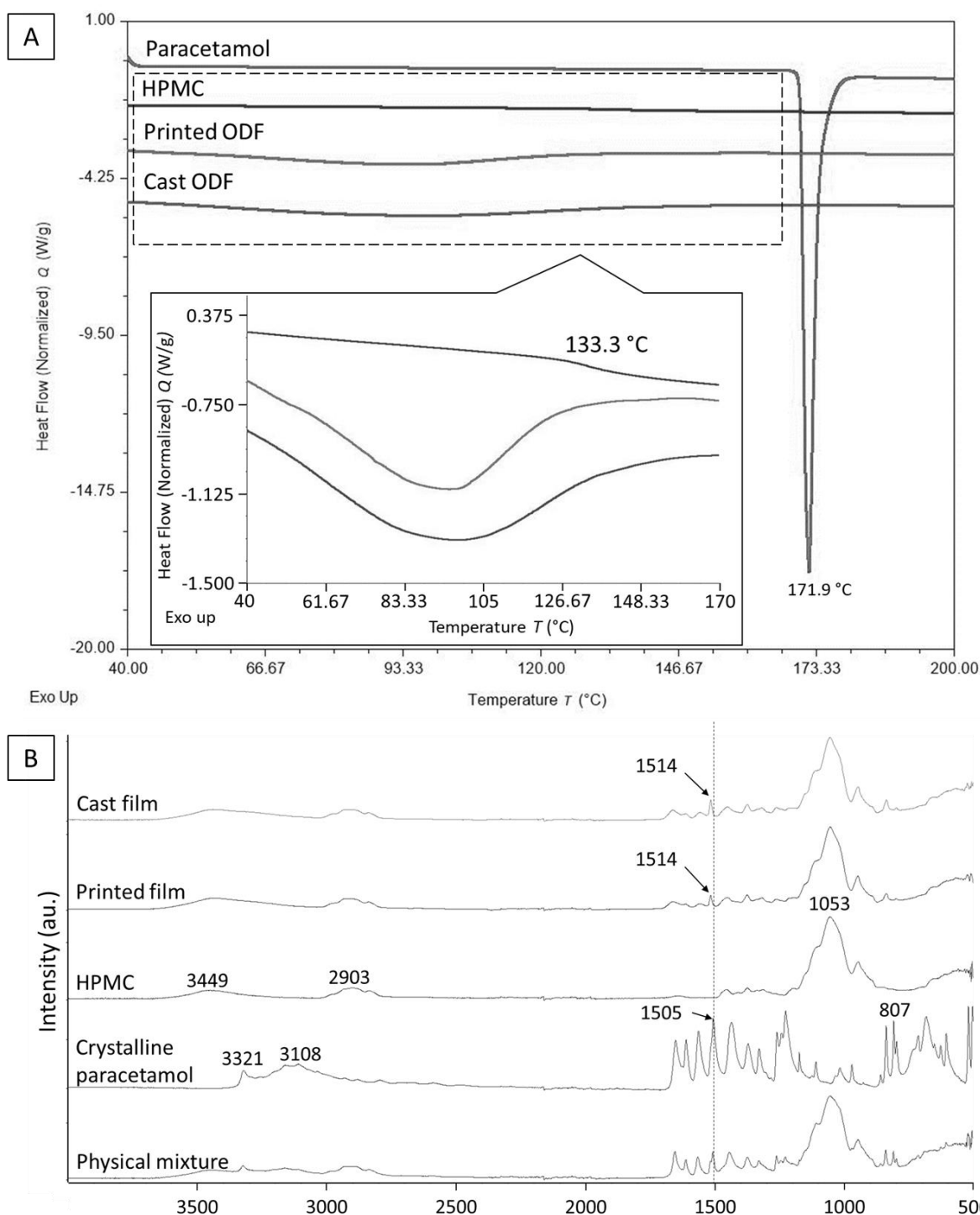
542

Fig. 7. *(A) DSC thermograms and (B) ATR-FTIR spectra of the raw materials, the cast drug loaded ODFs and MD printed drug loaded ODFs with eight printing cycles.*

3.7. Mechanical properties of drug loaded ODFs

The ODFs have to be strong enough to be handled during the manufacturing process, the packaging process and the administration to patients (Wasilewska and Winnicka, 2019).

550 Literature suggested that ODFs with a tensile strength higher than 2 N/mm^2 and an elongation

551 at break of more than 10 % are preferable to demonstrate good handling properties (Visser et

552 al., 2015). However, there is no official specifications on such parameters are available.

553 Therefore, in this study, the commercially available Listerine PocketPaks® ODFs was used as

554 the benchmark comparison to assess the handling properties of the ODFs prepared by MD

555 printing and casting. As Listerine PocketPaks® ODFs is a marketed product and is produced

556 commercially, we assume the product provide sufficient mechanical properties for production,

557 packaging and handling.

558

559 **Fig. 8** shows the mechanical test of MD printed and cast drug loaded ODFs in comparison to

560 the Listerine PocketPaks® ODFs. It is worth noting that for MD printed films the break points

561 were mostly close to the contact point with the clamps, whereas for the cast films, some broke

562 in the middle and others broke close to the contact point with the clamps. The likely cause of

563 the breaking points of the MD printed films being closer to the clamps is the lower thickness

564 of the edges than the centres, as illustrated in **Fig. 5B**. The tensile strength and elongation at

565 break for Listerine PocketPaks® films were 29.29 ± 2.39 N/mm^2 and 0.99 ± 0.14 %,

566 respectively; both parameters were statistically significantly lower than the cast (p = 0.008 <

567 0.05. and p = 0.001 < 0.05) and MD printed ODFs (p = 0.008 < 0.05. and p = 0.001 < 0.05).

568 Although the Listerine PocketPaks® use pullulan as the main film-forming polymer, the

569 thickness of Listerine PocketPaks® films are very similar to the MD printed films (see **Fig. 5B**).

570 As the film thickness has a significant effect on the mechanical properties, it is reasonable to

571 direct compare the mechanical properties of the MD printed film and Listerine PocketPaks®.

572 The results imply that the MD printed drug loaded ODFs have better handling properties than

573 Listerine PocketPaks® ODFs. The tensile strength of the 18 mm x 18 mm MD printed ODFs

574 and cast ODFs were 60.39 ± 7.43 N/mm^2 and 53.27 ± 2.19 N/mm^2 respectively, which shows

575 no statistical difference (p = 0.115 > 0.05). The percentage elongation for the MD printed ODFs

576 and cast ODFs were 2.50 ± 0.47 % and 7.00 ± 1.51 %, respectively, showing a significant

577 statistical difference (p = 0.001 < 0.05). The difference seen in the elongation between cast and

578 MD printed drug loaded ODFs could be due to the difference in the uniformity in thickness of

579 the films made by the two methods. The cast films have highly uniform thickness because they

580 were cut from the centre of a large parent film, whereas the MD printed films were individually

581 printed with no wastage, but the edges of the films that are directly in contact with the clamps

582 of the texture analyser sample holder were thinner than the centres of the films, and therefore

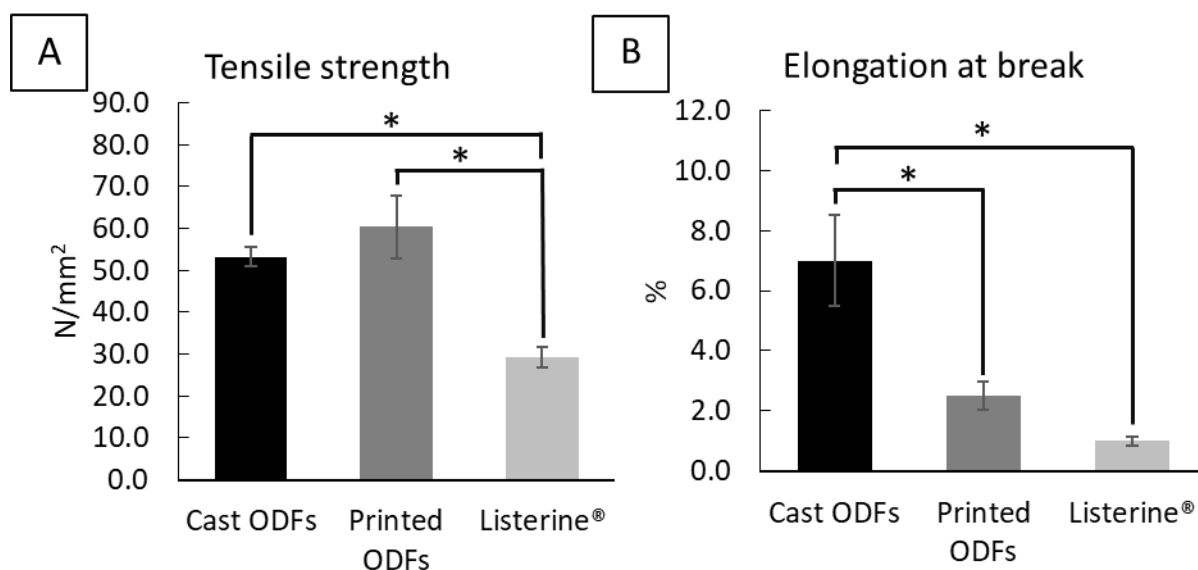583 offered a lower cross-sectional area.

584

Fig. 8. Mechanical properties of drug loaded ODFs prepared by casting and MD printing, and Listerine PocketPak® films: (A) tensile strength measurements and (B) elongation (%) at break. Asterisks refer to a statistically significant difference with cast film.

588

3.8. Drug content uniformity in MD printed ODFs

The relationship between the dispensed drug within the MD printed ODFs and the number of printing cycles ranging from 1 to 8 is shown in **Fig. 9A**. The number of printing cycles showed a highly linear relationship with the amount of paracetamol loaded into the ODFs with an excellent correlation coefficient (R^2 = 0.995). When the drug quantity in **Table 3** being converted into percentage (% w/w) drug loading (drug content/dry film weight x 100%), with changing the number of printing cycles, the paracetamol loading concentration (% w/w) of the MD printed ODFs remained relatively constant, ranged from 7.89 to 7.27 % w/w. Taking the paracetamol concentration in cast ODF (7.63% w/w) as the benchmark, the concentration difference is less than 0.36%. According to the literature, the drug content uniformity of ODFs is suggested to be within 85 – 115% of the average drug content (Ph.Eur. 2013, Dixit and Puthli, 2009). The drug contents of all MD printed ODFs fall well within this range. This result indicates a low inter-drop volume variance of the MD printing process. The high accuracy in drop volume and the reproducibility of the printing allows the MD printing to be used as a small-batch manufacturing process to produce ODFs with adjustable doses by simply changing the number of printing cycles.
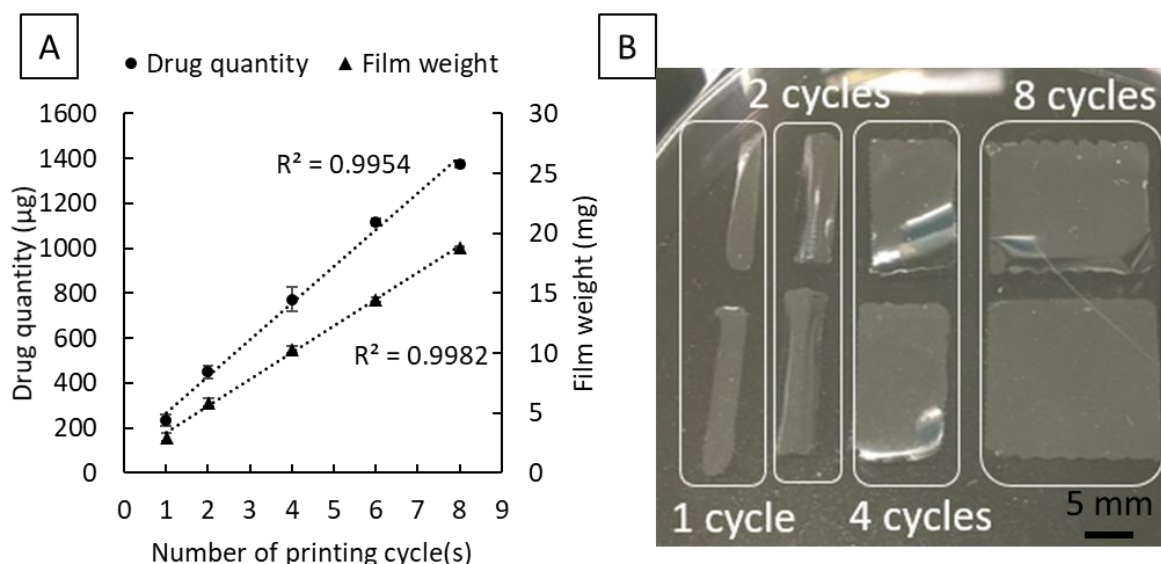
605

25

Fig. 9. *(A) The correlations between the drug loading and the overall film weight of the*

ODFs prepared by MD printing with the numbers of printing cycles; (B) digital photography

of the MD printed ODFs with different printing cycles.

3.9. Disintegration behaviour of drug loaded ODFs prepared by MD printing

The disintegration times of drug loaded ODFs prepared by casting and MD printing are reported in **Table 3.** The disintegration time of the MD printed films (8 printing cycles) and the cast films are 29.0 ± 3.6 s and 30.0 ± 3.6 s, respectively. There is no statistical significance exhibited by the MD printed (8 printing cycles) and the cast films. When comparing the disintegration time among different printing cycles, the results show no statistical difference either by One-way ANOVA test. Disintegration time is one of the critical factors to be considered in the manufacturing of ODFs. However, there is no specific monography for the disintegration time for ODF film. The monography of oral dispersible tablets was adopted as a guide. The European Pharmacopeia suggested 3 minutes as the target disintegration time (Ph.Eur., 2013). The FDA stated that oral dispersible tablets' disintegration time is lower than 30 s in water (FDA, 2008). The printed ODFs were able to fulfil the criteria set by European Pharmacopeia. It has been reported in the literature that the thickness of ODFs can significantly affect the disintegration time (Zhang et al., 2018). Although the overall thickness of the drug loaded ODFs prepared by MD printing (8 printing cycles) and casting showed a statistical difference, it may not be significant enough to show a significant difference in disintegration time. The fast disintegration led to rapid and complete dissolution of the film within 5 minutes with 100% drug release.

630 The number of printing cycles is independent of the disintegration time which is the time taken
631 for the film to disintegrate, but not completely dissolve. This is likely because the film thickness
632 of all the MD printed films remained mainly between 50 - 60 µm (data not shown). Although
633 the film dimension increases with printing cycles, the thickness of the film is likely to be the
634 dominating factor for controlling the disintegration time of the film.
635
636 **3.10. Analysis of MD printing as a manufacturing method for drug loaded ODFs**
637 The concept of individualised medicine was suggested to benefit patients by delivering an
638 appropriate amount of API to avoid adverse side effects and improve patient compliance. The
639 data presented in this study suggested that a MD system could fit well to the point-of-care
640 production of personalised medicine on-demand model for ODFs products. The major
641 advantages of MD printing over inkjet printing are being able to operate on viscous liquid
642 formulations and produce substrate-free ODFs. ODFs prepared by inkjet printing require an
643 edible substrate to absorb the drug ink (Genina et al., 2013; Sandler et al., 2011), which is
644 unnecessary for ODFs prepared by MD. Absorption kinetic and thermodynamic changes
645 according to the solvent used in ink and the substrate, increasing the manufacturing process's
646 complexity (Sandler et al., 2011). Inkjet printing ink formulation containing low polymer
647 concentration with high drug concentration is a strategy to overcome low drug loading per drop
648 (Vuddanda et al., 2018). However, the high risk of drug recrystallisation over time in the course
649 of printing should not be ignored in such liquid formulations with high drug loading. The
650 accumulation of drug crystals and small nozzle used for inkjet printhead increases the
651 likelihood of nozzle blockage, which is less likely for the MD since a bigger nozzle is used to
652 deposit viscous ink. MD can also dispense lipid-based formulations such as emulsion to
653 enhance the drug loading of poorly water-soluble drugs in ODFs, which is another advantage
654 compared to inkjet printing.
655
656 In terms of the feasibility of the manufacturing process, first, the polymer-drug inks with fixed
657 drug concentrations could be centrally prepared in pharmaceutical manufacturing plants with
658 GMP standards. The standardised inks can be distributed to the point of care manufacturing
659 sites, such as hospital pharmacies, to be printed by a MD system in a clean environment to
660 produce tailored doses of ODFs on-demand for patients. Scaling up the manufacturing would
661 be possible by using multiple print heads simultaneously to increase the production volume.
662
663 **4. Conclusion**

Overall, on-demand additive printing of fast dissolving ODFs with various doses of paracetamol was demonstrated by the MD system. A viscous polymer-drug ink was used to enable single-pass printing to fabricate ODFs with sufficient thickness for good handling. The dose of paracetamol in ODFs was adjustable linearly by printing ODFs with different printing cycles to change the print area. The deposition of droplets was sequenced to have sufficient overlapping to produce solid ODFs. The surface morphology of printed ODFs was comparable to the cast ODFs, showing a smooth surface without any bubbles. Although the mechanical properties of printed ODFs were statistically different from the cast film, the disintegration time was similar for both fabrication methods. The MD system is designed for depositing viscous liquid with high accuracy, which is suitable for fabricating tailored dose ODFs on-demand. The MD system can avoid issues such as blocked nozzle and recrystallisation of API, which can be an issue for ODFs prepared by inkjet printing. The results of this study demonstrated that the MD printing is an accurate liquid dispensing method for viscous fluids, and it has a wider range of potential applications beyond ODFs manufacturing, such as in personalised liquid dispensing and coating of devices.

Reference

Al-Zoubi, N., Koundourellis, J.E., Malamataris, S., 2002. FT-IR and Raman spectroscopic methods for identification and quantitation of orthorhombic and monoclinic paracetamol in powder mixes. J. Pharm. Biomed. Anal. 29, 459–467. https://doi.org/10.1016/S0731-7085(02)00098-5

Alhayali, A., Vuddanda, P.R., Velaga, S., 2019. Silodosin oral films: Development, physico-mechanical properties and in vitro dissolution studies in simulated saliva. J. Drug Deliv. Sci. Technol. 53, 101122. https://doi.org/10.1016/j.jddst.2019.06.019

Bonhoeffer, B., Kwade, A., Juhnke, M., 2018. Alternative Manufacturing Concepts for Solid Oral Dosage Forms From Drug Nanosuspensions Using Fluid Dispensing and Forced Drying Technology. J. Pharm. Sci. 107, 909–921. https://doi.org/10.1016/j.xphs.2017.11.007

Bonhoeffer, B., Kwade, A., Juhnke, M., 2017. Impact of Formulation Properties and Process Parameters on the Dispensing and Depositioning of Drug Nanosuspensions Using Micro-Valve Technology. J. Pharm. Sci. 106, 1102–1110. https://doi.org/10.1016/j.xphs.2016.12.019

Borges, A.F., Silva, C., Coelho, J.F.J., Simões, S., 2015. Oral films: Current status and future perspectives II-Intellectual property, technologies and market needs. J. Control. Release

698   206, 108–121. https://doi.org/10.1016/j.jconrel.2015.03.012

699   Cader, H.K., Rance, G.A., Alexander, M.R., Gonçalves, A.D., Roberts, C.J., Tuck, C.J.,

700   Wildman, R.D., 2019. Water-based 3D inkjet printing of an oral pharmaceutical dosage

701   form. Int. J. Pharm. 564, 359–368. https://doi.org/10.1016/j.ijpharm.2019.04.026

702   Chonkar, A.D., Rao, J.V., Managuli, R.S., Mutalik, S., Dengale, S., Jain, P., Udupa, N., 2016.

703   Development of fast dissolving oral films containing lercanidipine HCl nanoparticles in

704   semicrystalline polymeric matrix for enhanced dissolution and ex vivo permeation. Eur.

705   J. Pharm. Biopharm. 103, 179–191. https://doi.org/10.1016/j.ejpb.2016.04.001

706   Dixit, R.P., Puthli, S.P., 2009. Oral strip technology: Overview and future potential. J.

707   Control. Release 139, 94–107. https://doi.org/10.1016/j.jconrel.2009.06.014

708   Edinger, M., Bar-Shalom, D., Sandler, N., Rantanen, J., Genina, N., 2018a. QR encoded

709   smart oral dosage forms by inkjet printing. Int. J. Pharm. 536, 138–145.

710   https://doi.org/10.1016/j.ijpharm.2017.11.052

711   Edinger, M., Jacobsen, J., Bar-Shalom, D., Rantanen, J., Genina, N., 2018b. Analytical

712   aspects of printed oral dosage forms. Int. J. Pharm. 553, 97–108.

713   https://doi.org/10.1016/j.ijpharm.2018.10.030

714   Ehtezazi, T., Algellay, M., Islam, Y., Roberts, M., Dempster, N.M., Sarker, S.D., 2018. The

715   Application of 3D Printing in the Formulation of Multilayered Fast Dissolving Oral

716   Films. J. Pharm. Sci. 107, 1076–1085. https://doi.org/10.1016/j.xphs.2017.11.019

717   FDA, 2008. Guidance for Industry Orally Disintegrating Tablets [WWW Document]. URL

718   https://www.fda.gov/regulatory-information/search-fda-guidance-documents/orally-

719   disintegrating-tablets (accessed 7.29.21).

720   Foo, W.C., Khong, Y.M., Gokhale, R., Chan, S.Y., 2018. A novel unit-dose approach for the

721   pharmaceutical compounding of an orodispersible film. Int. J. Pharm. 539, 165–174.

722   https://doi.org/10.1016/j.ijpharm.2018.01.047

723   Genina, N., Janßen, E.M., Breitenbach, A., Breitkreutz, J., Sandler, N., 2013. Evaluation of

724   different substrates for inkjet printing of rasagiline mesylate. Eur. J. Pharm. Biopharm.

725   85, 1075–1083. https://doi.org/10.1016/j.ejpb.2013.03.017

726   Gupta, M.S., Kumar, T.P., Gowda, D.V., 2020. Orodispersible Thin Film: A new patient-

727   centered innovation. J. Drug Deliv. Sci. Technol. 59, 101843.

728   https://doi.org/10.1016/j.jddst.2020.101843

729   Hoffmann, E.M., Breitenbach, A., Breitkreutz, J., 2011. Advances in orodispersible films for

730   drug delivery. Expert Opin. Drug Deliv. 8, 299–316.

731   https://doi.org/10.1517/17425247.2011.553217

732   Hutchings, I.M., Martin, G. (Graham D.T.A.-T.T.-, 2013. Inkjet technology for digital

733   fabrication, NV-1 onl. ed. Wiley, Chichester, West Sussex, United Kingdom.

734   Karki, S., Kim, H., Na, S.J., Shin, D., Jo, K., Lee, J., 2016. Thin films as an emerging

735   platform for drug delivery. Asian J. Pharm. Sci. 11, 559–574.

736   https://doi.org/10.1016/j.ajps.2016.05.004

737   Low, A.Q.J., Parmentier, J., Khong, Y.M., Chai, C.C.E., Tun, T.Y., Berania, J.E., Liu, X.,

738   Gokhale, R., Chan, S.Y., 2013. Effect of type and ratio of solubilising polymer on

739   characteristics of hot-melt extruded orodispersible films. Int. J. Pharm. 455, 138–147.

740   https://doi.org/10.1016/j.ijpharm.2013.07.046

741   Morales, J.O., McConville, J.T., 2011. Manufacture and characterization of mucoadhesive

742   buccal films. Eur. J. Pharm. Biopharm. 77, 187–199.

743   https://doi.org/10.1016/j.ejpb.2010.11.023

744   Musazzi, U.M., Khalid, G.M., Selmin, F., Minghetti, P., Cilurzo, F., 2020. Trends in the

745   production methods of orodispersible films. Int. J. Pharm. 576.

746   https://doi.org/10.1016/j.ijpharm.2019.118963

747   Musazzi, U.M., Selmin, F., Ortenzi, M.A., Mohammed, G.K., Franzé, S., Minghetti, P.,

748   Cilurzo, F., 2018. Personalized orodispersible films by hot melt ram extrusion 3D

749   printing. Int. J. Pharm. 551, 52–59. https://doi.org/10.1016/j.ijpharm.2018.09.013

750   Öblom, H., Sjöholm, E., Rautamo, M., Sandler, N., 2019. Towards printed pediatric

751   medicines in hospital pharmacies: Comparison of 2d and 3d-printed

752   orodispersiblewarfarin films with conventional oral powders in unit dose sachets.

753   Pharmaceutics 11. https://doi.org/10.3390/pharmaceutics11070334

754   Pardeike, J., Strohmeier, D.M., Schrödl, N., Voura, C., Gruber, M., Khinast, J.G., Zimmer,

755   A., 2011. Nanosuspensions as advanced printing ink for accurate dosing of poorly

756   soluble drugs in personalized medicines. Int. J. Pharm. 420, 93–100.

757   https://doi.org/10.1016/j.ijpharm.2011.08.033

758   Ph.Eur., 2013. European Pharmacopoeia Version 8. 8.

759   Planchette, C., Pichler, H., Wimmer-Teubenbacher, M., Gruber, M., Gruber-Woelfler, H.,

760   Mohr, S., Tetyczka, C., Hsiao, W.K., Paudel, A., Roblegg, E., Khinast, J., 2016. Printing

761   medicines as orodispersible dosage forms: Effect of substrate on the printed micro-

762   structure. Int. J. Pharm. 509, 518–527. https://doi.org/10.1016/j.ijpharm.2015.10.054

763   Preis, M., Breitkreutz, J., Sandler, N., 2015. Perspective: Concepts of printing technologies

764   for oral film formulations. Int. J. Pharm. 494, 578–584.

765   https://doi.org/10.1016/j.ijpharm.2015.02.032

766 Preis, M., Knop, K., Breitkreutz, J., 2014. Mechanical strength test for orodispersible and

767   buccal films. Int. J. Pharm. 461, 22–29. https://doi.org/10.1016/j.ijpharm.2013.11.033

768 Repka, M.A., Gutta, K., Prodduturi, S., Munjal, M., Stodghill, S.P., 2005. Characterization of

769   cellulosic hot-melt extruded films containing lidocaine. Eur. J. Pharm. Biopharm. 59,

770   189–196. https://doi.org/10.1016/j.ejpb.2004.06.008

771 Sandler, N., Määttänen, A., Ihalainen, P., Kronberg, L., Meierjohann, A., Viitala, T.,

772   Peltonen, J., 2011. Inkjet printing of drug substances and use of porous substrates-

773   towards individualized dosing. J. Pharm. Sci. 100, 3386–3395.

774   https://doi.org/10.1002/jps.22526

775 Sandler, N., Preis, M., 2016. Printed Drug-Delivery Systems for Improved Patient Treatment.

776   Trends Pharmacol. Sci. 37, 1070–1080. https://doi.org/10.1016/j.tips.2016.10.002

777 Scoutaris, N., Ross, S., Douroumis, D., 2016. Current Trends on Medical and Pharmaceutical

778   Applications of Inkjet Printing Technology. Pharm. Res. 33, 1799–1816.

779   https://doi.org/10.1007/s11095-016-1931-3

780 Sibik, J., Sargent, M.J., Franklin, M., Zeitler, J.A., 2014. Crystallization and phase changes in

781   paracetamol from the amorphous solid to the liquid phase. Mol. Pharm. 11, 1326–1334.

782   https://doi.org/10.1021/mp400768m

783 Slavkova, M., Breitkreutz, J., 2015. Orodispersible drug formulations for children and

784   elderly. Eur. J. Pharm. Sci. 75, 2–9. https://doi.org/10.1016/j.ejps.2015.02.015

785 Trenfield, S.J., Awad, A., Goyanes, A., Gaisford, S., Basit, A.W., 2018. 3D Printing

786   Pharmaceuticals: Drug Development to Frontline Care. Trends Pharmacol. Sci. 39, 440–

787   451. https://doi.org/10.1016/j.tips.2018.02.006

788 Vermes GmbH, 2020. The MDS 3000 Series [WWW Document]. URL

789   https://www.vermes.com/en/micro-dispensing-systems/mds-micro-dispensing-systems/

790   (accessed 7.5.21).

791 Visser, J.C., Dohmen, W.M.C., Hinrichs, W.L.J., Breitkreutz, J., Frijlink, H.W., Woerdenbag,

792   H.J., 2015. Quality by design approach for optimizing the formulation and physical

793   properties of extemporaneously prepared orodispersible films. Int. J. Pharm. 485, 70–76.

794   https://doi.org/10.1016/j.ijpharm.2015.03.005

795 Vuddanda, P.R., Alomari, M., Dodoo, C.C., Trenfield, S.J., Velaga, S., Basit, A.W.,

796   Gaisford, S., 2018. Personalisation of warfarin therapy using thermal ink-jet printing.

797   Eur. J. Pharm. Sci. 117, 80–87. https://doi.org/10.1016/j.ejps.2018.02.002

798 Wang, S.L., Lin, S.Y., Wei, Y.S., 2002. Transformation of metastable forms of

799   acetaminophen studied by thermal Fourier transform infrared (FT-IR)

800   microspectroscopy. Chem. Pharm. Bull. 50, 153–156.

801   https://doi.org/10.1248/cpb.50.153

802 Wasilewska, K., Winnicka, K., 2019. How to assess orodispersible film quality? A review of

803   applied methods and their modifications. Acta Pharm. 69, 155–176.

804   https://doi.org/10.2478/acph-2019-0018

805 Wickström, H., Palo, M., Rijckaert, K., Kolakovic, R., Nyman, J.O., Määttänen, A.,

806   Ihalainen, P., Peltonen, J., Genina, N., De Beer, T., Löbmann, K., Rades, T., Sandler, N.,

807   2015. Improvement of dissolution rate of indomethacin by inkjet printing. Eur. J. Pharm.

808   Sci. 75, 91–100. https://doi.org/10.1016/j.ejps.2015.03.009

809 Wong, Y.S., Sun, J., Loh, H.T., Fuh, Y.H., Xu, Q., Ng, J.H., 2009. Comparison of micro-

810   dispensing performance between micro-valve and piezoelectric printhead. Microsyst.

811   Technol. 15, 1437–1448. https://doi.org/10.1007/s00542-009-0905-3

812 Zhang, L., Aloia, M., Pielecha-Safira, B., Lin, H., Rajai, P.M., Kunnath, K., Davé, R.N.,

813   2018. Impact of Superdisintegrants and Film Thickness on Disintegration Time of Strip

814   Films Loaded With Poorly Water-Soluble Drug Microparticles. J. Pharm. Sci. 107,

815   2107–2118. https://doi.org/10.1016/j.xphs.2018.04.006

816